Physics Letters B 785 (2018) 332–337

Contents lists available at ScienceDirect

Physics Letters B

www.elsevier.com/locate/physletb

Stochastic bias from loops of massive particles during inflation

Michael McAneny, Alexander K. Ridgway *, Mikhail P. Solon, Mark B. Wise

Walter Burke Institute for Theoretical Physics, California Institute of Technology, Pasadena, CA 91125, United States of America

ARTICLE INFO

Article history:
Received 3 January 2018
Received in revised form 8 June 2018
Accepted 9 June 2018
Available online 15 June 2018
Editor: H. Peiris

ABSTRACT

Primordial non-Gaussianities enhanced at small wavevectors can induce a power spectrum of the galaxy overdensity that differs greatly from that of the matter overdensity at large length scales. In previous work, it was shown that "squeezed" three-point and "collapsed" four-point functions of the curvature perturbation ζ can generate these non-Gaussianities and give rise to so-called scale-dependent and stochastic bias in the galaxy overdensity power spectrum. We explore a third way to generate non-Gaussianities enhanced at small wavevectors: the infrared behavior of quantum loop contributions to the four-point correlations of ζ. We show that these loop effects can give the largest contributions to the four-point function of ζ in the collapsed limit and be observable in the context of quasi-single field inflation.

1. Introduction

The inflationary paradigm [1] proposes an era in the very early universe during which the energy density is dominated by vacuum energy and the universe undergoes exponential expansion. Such a period elegantly explains why the universe is close to flat and the near isotropy of the cosmic microwave background (CMB). It also provides a simple quantum mechanical mechanism for generating energy density perturbations which have an almost scale-invariant Harrison–Zel'dovich power spectrum.

The simplest inflation models consist of a single scalar field ϕ, called the inflaton, whose time-dependent vacuum expectation value drives the expansion of the universe. The quantum fluctuations in the Goldstone mode π associated with the breaking of time translation invariance by the inflaton [2] source the energy density fluctuations. In the simplest of these single field models, the density perturbations are very nearly Gaussian [3]. One way to generate measurable non-Gaussianities is to introduce a second field s that interacts with the inflaton field during the inflationary era. A simple realization of such a model is quasi-single field inflation (QSFI) [4].

These non-Gaussianities affect the correlation functions of biased tracers of the underlying matter distribution such as galaxies. It was first pointed out in [5] and [6] that the power spectrum of the galaxy overdensity can become greatly enhanced relative to the Harrison–Zel'dovich spectrum on large scales if the primordial mass density perturbations are non-Gaussian.[1] These enhancements are known as scale-dependent bias and stochastic bias and were systematically explored in the context of QSFI in [7] and [8].[2]

The enhancements studied in [5] and [6] result from tree-level contributions to the three- and four-point functions of π that are in their "squeezed" and "collapsed" limits. In this paper, we consider quantum loop contributions to the correlation functions of π which (in the same kinematic limits) can also give rise to these long-distance effects. These loops arise from virtual excitations of massive scalar fields that existed during inflation.[3] We find that the infrared region of loop integrals can induce sizable stochastic bias on large scales without introducing any scale-dependent bias. In section 2 we illustrate this loop effect using a higher dimension operator that would appear in a generic effective theory of multi-field inflation. In section 3 we show that the loop effect can be observable in the context of QSFI and estimate the distance scale at which the loop contribution to the galaxy power spectrum could exceed the usual Harrison–Zel'dovich one.

* Corresponding author.
E-mail address: aridgway@caltech.edu (A.K. Ridgway).

[1] We refer to these effects as "enhancements" even though for certain model parameters they can interfere destructively with the usual Gaussian primordial density fluctuations.

[2] By stochastic bias, we mean the difference between the collapsed trispectrum and the squeezed bispectrum squared; see for example Eq. (2.7) of [7]. This stochastic bias can depend on the scale.

[3] These quantum loop contributions are distinct from loop contributions coming from, for example, higher-order terms in a bias expansion (see [9]).

https://doi.org/10.1016/j.physletb.2018.06.026

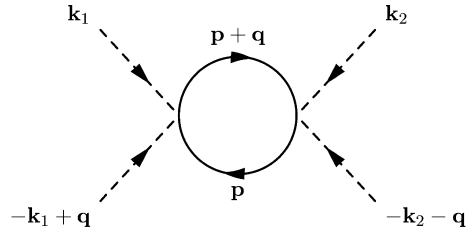

Fig. 1. One-loop contribution to the collapsed trispectrum of the primordial curvature perturbation. Dashed lines represent π, and solid lines represent s.

2. Loop-induced stochastic bias

Consider a theory of inflation that consists of two fields, the inflaton ϕ and a massive scalar s. Working in the gauge where $\phi(x)=\phi_0(t)$, the Lagrangian describing the Goldstone mode π due to the breaking of time translational invariance and s can be written as

$$\mathcal{L}=\frac{1}{2}g^{\mu\nu}\partial_\mu\pi\,\partial_\nu\pi+\frac{1}{2}g^{\mu\nu}\partial_\mu s\partial_\nu s-\frac{m^2}{2}s^2+\frac{1}{\Lambda^2}g^{\mu\nu}\partial_\mu\pi\,\partial_\nu\pi\,s^2+\ldots, \tag{2.1}$$

where the action is $S=\int d^4x\sqrt{-g}\mathcal{L}$. The dimension six operator in (2.1) induces the one-loop contribution to the four-point function of π depicted in Fig. 1. The complete theory includes additional interactions denoted by the ellipsis above [10,11],[4] which will give rise to other one-loop contributions that are comparable to or may even dominate this diagram. The goal of this section is to illustrate the infrared behavior of loop contributions to the correlation functions of π, which have interesting implications for the correlation functions of galaxies. For simplicity, we only consider the interaction given in (2.1) and leave a more complete study to future work.

We focus on the "collapsed" limit of the diagram, which occurs when the external wavevectors come in pairs that are nearly equal and opposite, as shown in Fig. 1 with $q\ll k_i$. This contribution to the four-point function has previously been computed in [12], where the role of conformal symmetry was emphasized. In this section, we review this calculation and describe its effect on the power spectrum of galaxy overdensities.

To begin, we express the quantum fields π and s in terms of creation and annihilation operators

$$\pi(\mathbf{x},\tau)=\int\frac{d^3k}{(2\pi)^3}a(\mathbf{k})\pi_k(\eta)e^{i\mathbf{k}\cdot\mathbf{x}}+\text{h.c.},$$
$$s(\mathbf{x},\tau)=\int\frac{d^3k}{(2\pi)^3}b(\mathbf{k})s_k(\eta)e^{i\mathbf{k}\cdot\mathbf{x}}+\text{h.c.}, \tag{2.2}$$

where $k=|\mathbf{k}|$, and $\eta=k\tau$ for conformal time $\tau<0$. The mode functions satisfy the equations of motion of the free theory with appropriate boundary conditions and are

$$\pi_k(\eta)=\frac{H}{k^{3/2}}\pi(\eta),\qquad \pi(\eta)=\frac{1}{\sqrt{2}}(1+i\eta)e^{-i\eta}, \tag{2.3}$$

$$s_k(\eta)=\frac{H}{k^{3/2}}s(\eta),\qquad s(\eta)=-ie^{i(2-\nu)\frac{\pi}{2}}\frac{\sqrt{\pi}}{2}(-\eta)^{3/2}H^{(1)}_{\frac{3}{2}-\nu}(-\eta), \tag{2.4}$$

where $\nu=3/2-\sqrt{9/4-m^2/H^2}$ and $H^{(1)}_z$ is the Hankel function of the first kind. We assume that the mass m of the field s is much less than the Hubble constant H during inflation, or equivalently $\nu\ll 1$.[5] We are interested in this region of parameter space because it leads to the largest infrared enhanced contributions to the four-point function.

Let us now compute the contribution in Fig. 1 to the collapsed trispectrum of the primordial curvature perturbation $\zeta=-(H/\dot\phi_0)\pi$. The primordial curvature trispectrum T_ζ is defined by

$$\langle\zeta_{\mathbf{k}_1}\zeta_{\mathbf{k}_2}\zeta_{\mathbf{k}_3}\zeta_{\mathbf{k}_4}\rangle_c=T_\zeta(\mathbf{k}_1,\mathbf{k}_2,\mathbf{k}_3,\mathbf{k}_4)(2\pi)^3\delta^3(\mathbf{k}_1+\mathbf{k}_2+\mathbf{k}_3+\mathbf{k}_4) \tag{2.5}$$

where the subscript c denotes the connected part of the four-point function. In Fig. 1 $\mathbf{k}_3=-\mathbf{k}_1+\mathbf{q}$ and $\mathbf{k}_4=-\mathbf{k}_2-\mathbf{q}$. The collapsed configuration $T_\zeta^{\rm coll}$ occurs when $q\ll k_i$.

Using the in-in formalism [13] and introducing the variables $\eta=k_1\tau$ and $\eta'=k_2\tau'$ we find

$$\begin{aligned}T_\zeta^{\rm coll}=\,&32\left(\frac{H}{\Lambda}\right)^4\left(\frac{H^2}{\dot\phi_0}\right)^4\frac{1}{k_1^3k_2^3}\int\frac{d^3p}{(2\pi)^3}\frac{1}{|\mathbf{p}+\mathbf{q}|^3p^3}\\&\times\int_{-\infty}^{0}\frac{d\eta}{\eta^2}\int_{-\infty}^{\frac{k_1}{k_2}\eta}\frac{d\eta'}{\eta'^2}e^{\epsilon(\eta+\eta')}\,\mathrm{Im}\left[F(\eta)\right]\\&\times\mathrm{Im}\left[F(\eta')s\left(\frac{|\mathbf{p}+\mathbf{q}|}{k_1}\eta\right)s^*\left(\frac{|\mathbf{p}+\mathbf{q}|}{k_2}\eta'\right)s\left(\frac{p}{k_1}\eta\right)\right.\\&\left.\times\,s^*\left(\frac{p}{k_2}\eta'\right)\right]+(k_1\leftrightarrow k_2)\end{aligned} \tag{2.6}$$

where

$$F(\eta)=\pi(0)^2\left([\partial_\eta\pi^*(\eta)]^2-[\pi^*(\eta)]^2\right). \tag{2.7}$$

In Eq. (2.6), ϵ is an infinitesimal positive quantity that regulates the time integrations in the distant past and we have expanded in $q\ll k_i$.

The dominant contribution of the loop integral in (2.6) comes from $p\sim q$. Moreover, the time integrals are dominated at late times $\eta,\eta'\sim-1$. We can thus use the small η expansion of the s mode function

$$s(\eta)\overset{\eta\to0}{\simeq}b_1(-\eta)^\nu,\qquad |b_1|^2=2^{1-2\nu}\Gamma(3/2-\nu)^2/\pi\overset{\nu\to0}{\simeq}1/2 \tag{2.8}$$

to find

$$T_\zeta^{\rm coll}\simeq 8\left(\frac{H}{\Lambda}\right)^4\left(\frac{H^2}{\dot\phi_0}\right)^4\frac{1}{(k_1k_2)^{3+2\nu}}I_{2\nu}(q)\,J^2 \tag{2.9}$$

where

$$I_{2\nu}(q)=\int\frac{d^3p}{(2\pi)^3}\frac{1}{|\mathbf{p}+\mathbf{q}|^{3-2\nu}p^{3-2\nu}}\overset{\nu\to0}{\simeq}\frac{1}{2\pi^2}\frac{1}{\nu}q^{-3+4\nu}, \tag{2.10}$$

$$J=\int_{-\infty}^{0}\frac{d\eta}{\eta^2}e^{\epsilon\eta}(-\eta)^{2\nu}\mathrm{Im}\left[F(\eta)\right]=2^{-2-2\nu}\frac{\Gamma(2+2\nu)}{1-2\nu}\overset{\nu\to0}{\simeq}\frac{1}{4}. \tag{2.11}$$

In (2.10) we have kept only the term singular in ν as it goes to zero. Note that our result is finite because we focused on the relevant region $p\sim q\ll k_i$ and neglected the region of large loop momenta which is not as important in the limit $q\to0$. The UV

[4] For example, the interaction $2\dot\phi_0\partial_\tau\pi s^2/\Lambda^2$ will also appear.

[5] In (2.1), the mass m includes contributions from terms such as $(\dot\phi_0^2/\Lambda^2)s^2$. Tuning is required for $m\ll H$.

divergence due to the region of large loop momentum would be rendered finite by a counterterm.

Our final result for the four-point function of the curvature perturbation for $m \ll H$ and $q \ll k_i$ is

$$T_\zeta^{\rm coll} \simeq \frac{1}{4\pi^2}\frac{1}{\nu}\left(\frac{H}{\Lambda}\right)^4\left(\frac{H^2}{\dot\phi_0}\right)^4\frac{1}{k_1^3k_2^3q^3}\left(\frac{q^2}{k_1k_2}\right)^{2\nu}. \tag{2.12}$$

The factors of wavevector magnitudes in (2.12) essentially follow from the form of $s(\eta)$ expanded for small η in the limit $m \ll H$, and from dimensional analysis. For $m \ll H$ the four-point function is enhanced by $1/\nu \simeq 3H^2/m^2$. This arises because for small m/H the mode function $s(\eta)$ falls off slowly as the mode k redshifts outside the de Sitter horizon. Note also that there is no IR divergence in the loop integration since the s field is massive. Three- and four-point curvature fluctuations generated by loop effects have been considered in Refs. [14–17] using the δN formalism. It would be interesting to see if this method can reproduce (2.12).

For small q the dependence of T_ζ on q in eq. (2.12) is almost the same as would result from a tree graph that contributes to it, say from iterating twice the interaction vertex that arises from $\mathcal{L}_{\rm int} = g^{\mu\nu}\partial_\mu\pi\partial_\nu\pi s/\Lambda'$ in the Lagrange density. That is because for small m, the s propagator in de Sitter space goes roughly as $1/q^3$. This is very different from flat space. To illustrate this, consider the flat space equal time expectation value $\langle\pi_{\rm k_1}\pi_{\rm k_2}\pi_{\rm k_3}\pi_{\rm k_4}\rangle$ in the kinematic limit,[6] $k_j \gg q \gg m$. At small q, the loop contribution is q-independent while the tree diagram goes as $1/q$.

We now qualitatively discuss the effects of (2.12) on the galaxy power spectrum. To begin, the matter overdensity δ_R averaged over a spherical volume of radius R is related to the primordial curvature fluctuation via

$$\delta_R(\mathbf{k}) = \frac{2k^2}{5\Omega_m H_0^2}T(k)W_R(k)\zeta_{\mathbf{k}} \tag{2.13}$$

where $W_R(k)$ is the window function, $T(k)$ is the transfer function, Ω_m is the ratio of the matter density to the critical density today, and H_0 is the Hubble constant evaluated today.

We consider an expansion for the galaxy overdensity δ_h in terms of δ_R of the following form

$$\delta_h(\mathbf{x}) = b_1\delta_R(\mathbf{x}) + b_2(\delta_R^2(\mathbf{x}) - \sigma_R^2) + b_3(\delta_R^3(\mathbf{x}) - 3\delta_R(\mathbf{x})\sigma_R^2) + \dots, \tag{2.14}$$

where $\sigma_R^2 = \langle\delta_R(\mathbf{x})\delta_R(\mathbf{x})\rangle$ and the constants b_1, b_2, and b_3 are bias coefficients (for a more complete treatment, see [18]). The bias coefficients can be determined from data or computed using a specific model of galaxy halo formation that expresses the galaxy overdensity in terms of δ_R. The two-point function of the galaxy overdensity is then:

$$\begin{aligned}\langle\delta_h(\mathbf{x})\delta_h(\mathbf{y})\rangle = {} & b_1^2\,\langle\delta_R(\mathbf{x})\delta_R(\mathbf{y})\rangle + b_1b_2\Big(\Big\langle(\delta_R^2(\mathbf{x}) - \sigma_R^2)\delta_R(\mathbf{y})\Big\rangle \\ & + \Big\langle\delta_R(\mathbf{x})(\delta_R^2(\mathbf{y}) - \sigma_R^2)\Big\rangle\Big) \\ & + b_2^2\Big\langle(\delta_R^2(\mathbf{x}) - \sigma_R^2)(\delta_R^2(\mathbf{y}) - \sigma_R^2)\Big\rangle + \dots\end{aligned} \tag{2.15}$$

A similar expression could be derived for the galaxy-matter cross-correlation $\langle\delta_h(\mathbf{x})\delta_R(\mathbf{y})\rangle$.

Ignoring other contributions to the non-Gaussianities of ζ besides the one given in (2.12), the term proportional to b_2^2 in (2.15) yields a contribution to the galaxy power spectrum of the form $P_{hh}(q) \sim 1/q^{3-4\nu}$, but not to the galaxy-matter cross-correlation $P_{hm}(q)$. Hence this loop contributes to stochastic bias, but not to scale-dependent bias. Note that in the absence of primordial non-Gaussianity, $P_{hh}(q) \sim q$, so the trispectrum contribution is enhanced by a relative factor of $q^{-4+4\nu}$ and dominates as $q \to 0$.

It is worth emphasizing that we have only considered one particular interaction in this theory, and have ignored other interactions which may give even more important contributions to stochastic and scale-dependent bias. We now turn to a model within QSFI in order to make a full prediction in a consistent theory.

3. Loop-induced stochastic bias in quasi-single field inflation

In this section, we show that loop-induced non-Gaussianities in QSFI [4] can give rise to stochastic bias that is potentially observable given the stringent constraints from CMB data on non-Gaussianities. The model we consider consists of an inflaton ϕ and a massive scalar s with the symmetries $\phi \to \phi + c$, $\phi \to -\phi$, and $s \to -s$. These symmetries are broken by the potential of ϕ as well as by the lowest dimension operator that couples ϕ and s, $g^{\mu\nu}\partial_\mu\phi\partial_\nu\phi s/\Lambda$. The Lagrangian written in terms of the Goldstone mode π is

$$\begin{aligned}\mathcal{L} = {} & \frac{1}{2}g^{\mu\nu}\partial_\mu\pi\,\partial_\nu\pi\left(1 + \frac{2}{\Lambda}s\right) + \frac{1}{2}g^{\mu\nu}\partial_\mu s\partial_\nu s \\ & - \mu H\tau s\partial_\tau\pi - \frac{m^2}{2}s^2 - \frac{V^{(4)}}{4!}s^4\end{aligned} \tag{3.1}$$

where the kinetic mixing term is parameterized by the coupling $\mu = 2\dot\phi_0/\Lambda$ and we have ignored higher order terms in the potential for s. Similar to the previous section, we focus here on the region where $m \ll H$ and $\mu \ll H$, which gives the most significant long wavelength enhancement to the galaxy power spectrum.

Due to the kinetic mixing, π and s share a set of creation and annihilation operators:

$$\begin{aligned}\pi(\mathbf{x},\tau) = {} & \int\frac{d^3k}{(2\pi)^3}\Big(a^{(1)}(\mathbf{k})\pi_k^{(1)}(\eta)e^{i\mathbf{k}\cdot\mathbf{x}} + a^{(2)}(\mathbf{k})\pi_k^{(2)}(\eta)e^{i\mathbf{k}\cdot\mathbf{x}} \\ & + \text{h.c.}\Big)\end{aligned} \tag{3.2}$$

$$\begin{aligned}s(\mathbf{x},\tau) = {} & \int\frac{d^3k}{(2\pi)^3}\Big(a^{(1)}(\mathbf{k})s_k^{(1)}(\eta)e^{i\mathbf{k}\cdot\mathbf{x}} + a^{(2)}(\mathbf{k})s_k^{(2)}(\eta)e^{i\mathbf{k}\cdot\mathbf{x}} \\ & + \text{h.c.}\Big)\,.\end{aligned} \tag{3.3}$$

The mode functions $\pi_k^{(i)} = (H/k^{3/2})\pi^{(i)}$ and $s_k^{(i)} = (H/k^{3/2})s^{(i)}$ are difficult to solve for exactly. However, analytic progress can be made by considering series solutions. It can easily be checked that the most general series solutions to the mode equations derived from (3.1) are

$$\begin{aligned}\pi^{(i)}(\eta) = {} & \sum_{n=0}^{\infty}\Big[a_{0,2n}^{(i)}(-\eta)^{2n} + a_{-,2n}^{(i)}(-\eta)^{2n+\alpha_-} + a_{+,2n}^{(i)}(-\eta)^{2n+\alpha_+} \\ & + a_{3,2n}^{(i)}(-\eta)^{2n+3}\Big]\end{aligned} \tag{3.4}$$

$$\begin{aligned}s^{(i)}(\eta) = {} & \sum_{n=0}^{\infty}\Big[b_{0,2n}^{(i)}(-\eta)^{2n} + b_{-,2n}^{(i)}(-\eta)^{2n+\alpha_-} + b_{+,2n}^{(i)}(-\eta)^{2n+\alpha_+} \\ & + b_{3,2n}^{(i)}(-\eta)^{2n+3}\Big]\end{aligned} \tag{3.5}$$

where $\alpha_\pm = 3/2 \pm \sqrt{9/4 - \mu^2/H^2 - m^2/H^2}$ and $b_{0,0}^{(i)} = 0$. For ease of notation we denote $a_{r,0}^{(i)}$ and $b_{r,0}^{(i)}$ as $a_r^{(i)}$ and $b_r^{(i)}$. In Ref. [8], it

[6] Because of time translation invariance in flat space this expectation value is independent of the time the fields π are evaluated at.

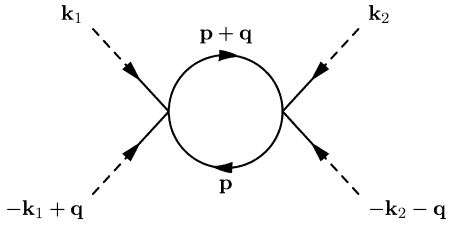

Fig. 2. One-loop contribution to the collapsed trispectrum of the primordial curvature perturbation in QSFI. Dashed lines represent π, and solid lines represent s.

was shown that the non-Gaussianities can be well approximated by a finite set of combinations of the power series coefficients when $\mu, m \ll H$. The combinations of power series coefficients needed to compute the loop in Fig. 2 are

$$\mathrm{Re}\left[a_0^{(i)} b_-^{*(i)}\right] \simeq \frac{-3\mu H}{2(\mu^2+m^2)}\,, \quad \mathrm{Im}\left[a_0^{(i)} b_3^{*(i)}\right] = \frac{\mu H}{2(\mu^2+m^2)}\,,$$
$$\left|b_-^{(i)}\right|^2 \simeq \frac{1}{2}\,, \tag{3.6}$$

$$\mathrm{Im}\left[a_0^{(i)} b_-^{*(i)}\right] = \mathrm{Im}\left[a_0^{(i)} b_{0,2}^{*(i)}\right] = \mathrm{Im}\left[a_0^{(i)} b_{-,2}^{*(i)}\right] = \mathrm{Im}\left[a_0^{(i)} b_+^{*(i)}\right] = 0\,, \tag{3.7}$$

which were determined in [8]. The repeated superscripts (i) are summed over $i = 1, 2$. The above expressions are valid for μ/H, $m/H \ll 1$.

We can now compute the loop contribution to the collapsed limit of the curvature perturbation trispectrum shown in Fig. 2. Again, using the in-in formalism and the variables $\eta = k_1\tau$ and $\eta' = k_2\tau'$, we find

$$\begin{aligned} T_\zeta^{\mathrm{coll}} = {} & 2V^{(4)2}\left(\frac{H^2}{\dot\phi_0}\right)^4 \frac{1}{k_1^3 k_2^3}\int \frac{d^3p}{(2\pi)^3}\frac{1}{|\mathbf{p}+\mathbf{q}|^3 p^3} \\ & \times \int_{-\infty}^{0}\frac{d\eta}{\eta^4}\int_{-\infty}^{\frac{k_1}{k_2}\eta}\frac{d\eta'}{\eta'^4}\mathrm{Im}\left[\left(\pi^{(i)}(0)s^{*(i)}(\eta)\right)^2\right] \\ & \times \mathrm{Im}\left[\left[\pi^{(j)}(0)s^{*(j)}(\eta')\right]^2 s^{(k)}\left(\frac{|\mathbf{p}+\mathbf{q}|}{k_1}\eta\right)\right. \\ & \left.\times\, s^{*(k)}\left(\frac{|\mathbf{p}+\mathbf{q}|}{k_2}\eta'\right)s^{(l)}\left(\frac{p}{k_1}\eta\right)s^{*(l)}\left(\frac{p}{k_2}\eta'\right)\right] \\ & + \left(k_1 \leftrightarrow k_2\right). \end{aligned} \tag{3.8}$$

Similar to before, the dominant contribution to the loop integral occurs for loop momenta $p \sim q \ll k_i$ and the time integrals are dominated by late times. We can immediately expand the s mode functions to find

$$T_\zeta^{\mathrm{coll}} \simeq \frac{1}{2}V^{(4)2}\left(\frac{H^2}{\dot\phi_0}\right)^4 \frac{1}{(k_1k_2)^{3+2\alpha_-}} I_{2\alpha_-}(q) K(\mu,m)^2\,, \tag{3.9}$$

where $I_\nu(q)$ is given in (2.10) and

$$K(\mu,m) = \int_{-\infty}^{0} d\eta(-\eta)^{-4+2\alpha_-}\mathrm{Im}\left[\left(\pi^{(i_1)}(0)s^{*(i_1)}(\eta)\right)^2\right]. \tag{3.10}$$

It was shown in [8] that the most important contribution to (3.10) is obtained by cutting off the lower bound of the integral at η_0 which is around horizon crossing. Inserting the power series expansions of the mode functions in (3.4) and (3.5), we find

$$\begin{aligned} K(\mu,m) &\simeq 2\,\mathrm{Im}\left[a_0^{(i)}b_3^{*(i)}\right]\mathrm{Re}\left[a_0^{(j)}b_-^{*(j)}\right]\int_{\eta_0}^{0} d\eta(-\eta)^{-1+3\alpha_-} \\ &\simeq -\frac{2}{3}\frac{(3\mu/2)^2H^4}{(\mu^2+m^2)^3}\,, \end{aligned} \tag{3.11}$$

where we have neglected contributions from higher powers of η which are suppressed in the limit $\alpha_- \ll 1$. Note that this piece most singular in α_- is insensitive to the choice of η_0. Our final result for the four-point function of the curvature perturbation for $m, \mu \ll H$ and $q \ll k_i$ is then

$$T_\zeta^{\mathrm{coll}} \simeq \frac{1}{3\pi^2}V^{(4)2}\left(\frac{H^2}{\dot\phi_0}\right)^4 \frac{1}{k_1^3k_2^3q^3}\left(\frac{q^2}{k_1k_2}\right)^{2\alpha_-}\frac{(3\mu/2)^4H^{10}}{(\mu^2+m^2)^7}\,. \tag{3.12}$$

In (3.12), the factors of wavevector magnitudes and α_-^{-1} from the integral $I_{2\alpha_-}$ are the same as those in (2.12) from the integral $I_{2\nu}$. These features are characteristic of quantum mechanical effects from the exchange of a massive particle [12,19]. In principle higher loop contributions have q scaling similar to (3.12), but are suppressed because they also have additional factors of the small coupling constant $V^{(4)}$.

We now consider the long wavelength enhancement to the galaxy power spectrum resulting from this collapsed primordial trispectrum. In our numerical evaluation, we make the simplifying assumption that galaxies form at points in space at which the smoothed matter overdensity is greater than a threshold density at the time of collapse $\delta_c(a_{\mathrm{coll}})$, *i.e.* $n_h(\mathbf{x}) \propto \Theta_H\left(\delta_R(\mathbf{x}, a_{\mathrm{coll}}) - \delta_c(a_{\mathrm{coll}})\right) = \Theta_H\left(\delta_R(\mathbf{x}) - \delta_c\right)$, where $\delta_c \equiv \delta_c(a_{\mathrm{coll}})/D(a_{\mathrm{coll}})$.[7] We further assume that $\delta_c(a_{\mathrm{coll}}) = 1.686$ [20], all halos collapse instantaneously at redshift $z = 1.5$, and their number density does not evolve in time after collapse. This corresponds to a value of $\delta_c = 4.215$. The galaxy overdensity is defined by $\delta_h(\mathbf{x}) = (n_h(\mathbf{x}) - \langle n_h\rangle)/\langle n_h\rangle$. With this threshold collapse model, the bias coefficients are given by (see e.g. [21])

$$b_1 = \frac{e^{-\frac{\delta_c^2}{2\sigma_R^2}}}{\sqrt{2\pi}\sigma_R\langle n_h\rangle}\,, \quad b_2 = \frac{\delta_c}{\sigma_R}\frac{e^{-\frac{\delta_c^2}{2\sigma_R^2}}}{2!\sqrt{2\pi}\sigma_R^2\langle n_h\rangle}\,,$$
$$b_3 = \left(\frac{\delta_c^2}{\sigma_R^2}-1\right)\frac{e^{-\frac{\delta_c^2}{2\sigma_R^2}}}{3!\sqrt{2\pi}\sigma_R^3\langle n_h\rangle} \tag{3.13}$$

where $\langle n_h\rangle = \mathrm{erfc}\left(\delta_c/(\sqrt{2}\sigma_R)\right)/2$. We use the BBKS approximation to the transfer function [22] and the top-hat window function $W_R(k) = 3(\sin(kR) - kR\cos(kR))/(kR)^3$. Moreover, we take $R = 1.9$ Mpc/h as the smoothing scale, and numerically we find $\sigma_R = 3.62$.

The Fourier transform of $\langle\delta_R(\mathbf{x})\delta_R(\mathbf{y})\rangle$ gives the matter power spectrum $P_{mm}(q)$:

$$P_{mm}(q) = \left(\frac{2}{5\Omega_m H_0^2}\right)^2\left(\frac{H^2}{\dot\phi_0}\right)^2 C_2(\mu,m)T(q)^2 q\,, \tag{3.14}$$

[7] $\delta_R(\mathbf{x})$ is the linearly evolved matter overdensity today.

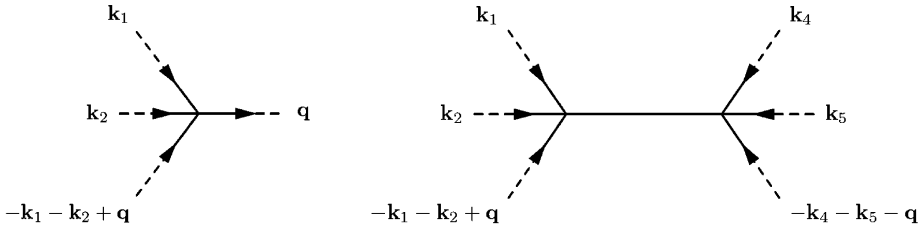

Fig. 3. These two tree-level diagrams involving the $V^{(4)}$ interaction can also contribute to scale-dependent and stochastic bias. However, these contributions are small compared to the loop contribution in Fig. 2 due a suppression arising from the integration over additional hard external wavevectors.

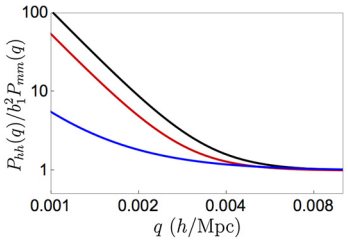

Fig. 4. The ratio $P_{hh}(q)/b_1^2P_{mm}(q)$ is plotted for $\tau_{NL}^{2\sigma}=2800$ (Planck 2013) in black, and $\tau_{NL}^{2\sigma}/2=1400$ in red. In blue, we plot the power spectrum ignoring the loop contribution and considering only the tree diagrams in Fig. 3, using the $\tau_{NL}^{2\sigma}$ bound. Note that the enhanced behavior begins around (200 Mpc/h)$^{-1}$ for the black curve, and around (300 Mpc/h)$^{-1}$ for the red curve. Moreover, note that the tree contributions in blue are very small compared to the loop contribution in black. We plot for $\mu/H=m/H=0.274$, corresponding to $\alpha_-=0.05$. Moreover we take $R=1.9$ Mpc/h and $\delta_c=4.215$ (For interpretation of the colors in the figure(s), the reader is referred to the web version of this article.).

where $C_2(\mu,m)=1/2+2(3\mu/2)^2H^2/(\mu^2+m^2)^2$ [8]. It then follows from (2.15) that the ratio of the galaxy power spectrum to the matter power spectrum normalized by b_1^2 is

$$\frac{P_{hh}(q)}{b_1^2P_{mm}(q)}=1+\frac{b_2^2}{b_1^2}\left(\frac{2}{5\Omega_mH_0^2R^2}\right)^2\left(\frac{H^2}{\dot\phi_0}\right)^2\frac{V^{(4)2}\mathcal{J}^2}{3\pi^2}\times\frac{(qR)^{-4+4\alpha_-}}{T(q)^2}\frac{(3\mu/2)^4H^{10}}{(\mu^2+m^2)^7C_2(\mu,m)} \tag{3.15}$$

where

$$\mathcal{J}=\frac{1}{2\pi^2}\int_0^\infty du\; T\,(u/R)^2\,W_R\,(u/R)^2\,u^3. \tag{3.16}$$

The $V^{(4)}$ interaction in (3.1) also gives rise to the tree-level diagrams shown in Fig. 3 which contribute to the long wavelength enhancement of the galaxy power spectrum. However, these terms contain integrals with three transfer functions rather than two like in (3.16). This integral then gives $\sim\mathcal{J}^{3/2}$ rather than $\mathcal{J}$. Numerically we find $\mathcal{J}\approx 3.1\times10^{-5}$ so the contributions from these tree-level diagrams are suppressed, as can be seen in Fig. 4.

One could also consider the contribution of the $(\partial\pi)^2s/\Lambda$ interaction in (3.1) to $P_{hh}(q)$. However, estimating $f_{NL}=5B_\zeta(k,k,k)/18P_\zeta(k)^2$ from this interaction numerically, we find that $f_{NL}\lesssim 10^{-2}$ for μ/H, $m/H\lesssim 0.4$. This small f_{NL} has a negligible contribution to $P_{hh}(q)$ compared to the loop contribution we have considered.

We can constrain $V^{(4)}$ using the bounds on τ_{NL} and g_{NL} from Planck 2013 and 2015 [23,24]. The bound due to τ_{NL} is estimated using (3.12), with factors of $(q/k)^{\alpha_-}$ set to 1 in order to match the τ_{NL} shape. The bound due to g_{NL} is estimated using the tree-level four-point diagram with a single $V^{(4)}$ vertex, with factors of $(k_i/k_j)^{\alpha_-}$ set to 1 to match the g_{NL} shape. We take $\tau_{NL}^{2\sigma}=2.8\times10^3$ and $g_{NL}^{2\sigma}=-2.44\times10^5$ as the maximum allowed values of τ_{NL} and g_{NL} at a 2σ confidence level. We find that for most of the (μ,m) parameter space $\tau_{NL}^{2\sigma}$ gives the stronger constraints on $V^{(4)}$. For $\mu/H=m/H=0.274$ (so that $\alpha_-=0.05$), we find that the $\tau_{NL}^{2\sigma}$ constraint yields $V^{(4)}\leq 0.014$.

In Fig. 4, we plot the ratio $P_{hh}(q)/b_1^2P_{mm}(q)$. The enhanced behavior begins at around $q\sim$ (200 Mpc/h)$^{-1}$ and $q\sim$ (300 Mpc/h)$^{-1}$ for the values of $V^{(4)}$ that saturate the $\tau_{NL}^{2\sigma}$ (black curve) and $\tau_{NL}^{2\sigma}/2$ (red curve) bounds. Moreover, the blue curve is the contribution due solely to the tree-level diagrams in Fig. 3 using the $\tau_{NL}^{2\sigma}$ bound, and is significantly smaller than the loop contribution shown in black.

Finally we briefly comment on how our results depend on the parameters R and δ_c. The loop contribution to $P_{hh}(q)/b_1^2P_{mm}(q)$ is insensitive to the choice of smoothing radius R. The tree-level contributions in Fig. 3 increase as R increases, yet even for $R=2.7$ Mpc/h, we find that the loop contribution remains an order of magnitude larger than the tree-level contributions. Furthermore, since $b_2/b_1\sim\delta_c$, the second term in (3.15) goes like $\delta_c^2/q^{4-4\alpha_-}$. This implies that the characteristic scale q_0 at which the long-wavelength enhancements become significant depends on δ_c like $q_0\sim\delta_c^{1/2}$.

4. Concluding remarks

Using a particular QSFI model, we have shown that one loop contributions to the four-point function of the curvature perturbation ζ in the collapsed limit can be even larger than the tree-level ones. In such cases the dominant contribution to stochastic bias at long wavelengths comes from primordial quantum loops. In this model, the one-loop contribution to the four-point function of primordial curvature perturbations induces a non-Gaussian contribution to the galaxy power spectrum $P_{hh}(q)$ that is five times larger than the Gaussian one at $q\sim h/(500$ Mpc) for values of τ_{NL} and g_{NL} at only half their current 2σ bounds. These non-Gaussianities could be observed in upcoming large-scale surveys [26,27,25].

It would be interesting to study the effects of these loop contributions to the bias within the framework of the effective field theory of inflation. At a minimum, this would require the computation of the one-loop diagram presented in section 2 and the ones due to the interaction $\mathcal{L}_I\sim\dot\pi s^2$.

Acknowledgements

This work was supported by the DOE Grant DE-SC0011632 and by the Walter Burke Institute for Theoretical Physics.

References

[1] A.A. Starobinsky, JETP Lett. 30 (1979) 682;
A. Guth, Phys. Rev. D 23 (1981) 347;
A.D. Linde, Phys. Lett. B 108 (1982) 389;
A.D. Linde, Phys. Lett. B 114 (1982) 431;
A. Albrecht, P. Steinhardt, Phys. Rev. Lett. 48 (1982) 1220.

[2] C. Cheung, P. Creminelli, A.L. Fitzpatrick, J. Kaplan, L. Senatore, J. High Energy Phys. 0803 (2008) 014, arXiv:0709.0293 [hep-th].
[3] J.M. Maldacena, J. High Energy Phys. 0305 (2003) 013, arXiv:astro-ph/0210603.
[4] X. Chen, Y. Wang, J. Cosmol. Astropart. Phys. 1004 (2010) 027, arXiv:0911.3380 [hep-th].
[5] T.J. Allen, B. Grinstein, M.B. Wise, Phys. Lett. B 197 (1987) 66.
[6] N. Dalal, O. Doré, D. Huterer, A. Shirokov, Phys. Rev. D 77 (2008) 123514, arXiv:0710.4560 [astro-ph].
[7] D. Baumann, S. Ferraro, D. Green, K.M. Smith, J. Cosmol. Astropart. Phys. 1305 (2013) 001, arXiv:1209.2173 [astro-ph.CO].
[8] H. An, M. McAneny, A.K. Ridgway, M.B. Wise, arXiv:1711.02667 [hep-ph].
[9] S. Yokoyama, T. Matsubara, Phys. Rev. D 87 (2013) 023525, https://doi.org/10.1103/PhysRevD.87.023525, arXiv:1210.2495 [astro-ph.CO].
[10] L. Senatore, M. Zaldarriaga, J. High Energy Phys. 1204 (2012) 024, https://doi.org/10.1007/JHEP04(2012)024, arXiv:1009.2093 [hep-th].
[11] N. Khosravi, J. Cosmol. Astropart. Phys. 1205 (2012) 018, https://doi.org/10.1088/1475-7516/2012/05/018, arXiv:1203.2266 [hep-th].
[12] N. Arkani-Hamed, J. Maldacena, arXiv:1503.08043 [hep-th].
[13] S. Weinberg, Phys. Rev. D 72 (2005) 043514, https://doi.org/10.1103/PhysRevD.72.043514, arXiv:hep-th/0506236.
[14] H.R.S. Cogollo, Y. Rodriguez, C.A. Valenzuela-Toledo, J. Cosmol. Astropart. Phys. 0808 (2008) 029, https://doi.org/10.1088/1475-7516/2008/08/029, arXiv:0806.1546 [astro-ph].
[15] Y. Rodriguez, C.A. Valenzuela-Toledo, Phys. Rev. D 81 (2010) 023531, https://doi.org/10.1103/PhysRevD.81.023531, arXiv:0811.4092 [astro-ph].
[16] J. Kumar, L. Leblond, A. Rajaraman, J. Cosmol. Astropart. Phys. 1004 (2010) 024, https://doi.org/10.1088/1475-7516/2010/04/024, arXiv:0909.2040 [astro-ph.CO].
[17] J. Bramante, J. Kumar, J. Cosmol. Astropart. Phys. 1109 (2011) 036, https://doi.org/10.1088/1475-7516/2011/09/036, arXiv:1107.5362 [astro-ph.CO].
[18] V. Desjacques, D. Jeong, F. Schmidt, arXiv:1611.09787 [astro-ph.CO].
[19] M. Mirbabayi, M. Simonović, J. Cosmol. Astropart. Phys. 1603 (03) (2016) 056, https://doi.org/10.1088/1475-7516/2016/03/056, arXiv:1507.04755 [hep-th].
[20] J.E. Gunn, J.R. Gott III, Astrophys. J. 176 (1972) 1, https://doi.org/10.1086/151605.
[21] S. Ferraro, K.M. Smith, D. Green, D. Baumann, Mon. Not. R. Astron. Soc. 435 (2013) 934, https://doi.org/10.1093/mnras/stt1272, arXiv:1209.2175 [astro-ph.CO].
[22] J.M. Bardeen, J.R. Bond, N. Kaiser, A.S. Szalay, Astrophys. J. 304 (1986) 15.
[23] P.A.R. Ade, et al., Planck Collaboration, Astron. Astrophys. 571 (2014) A24, https://doi.org/10.1051/0004-6361/201321554, arXiv:1303.5084 [astro-ph.CO].
[24] P.A.R. Ade, et al., Planck Collaboration, Astron. Astrophys. 594 (2016) A17, https://doi.org/10.1051/0004-6361/201525836, arXiv:1502.01592 [astro-ph.CO].
[25] O. Doré, et al., arXiv:1412.4872 [astro-ph.CO].
[26] P.A. Abell, et al., LSST Science and LSST Project Collaborations, arXiv:0912.0201 [astro-ph.IM].
[27] R. Laureijs, et al., EUCLID Collaboration, arXiv:1110.3193 [astro-ph.CO].